⌘ *Author's Choice*

THE JOURNAL OF BIOLOGICAL CHEMISTRY VOL. 287, NO. 1, pp. 438–445, January 2, 2012

Unifying Concept of Serotonin Transporter-associated Currents*[S]

Received for publication, September 20, 2011, and in revised form, October 20, 2011 Published, JBC Papers in Press, November 9, 2011, DOI 10.1074/jbc.M111.304261

Klaus Schicker[‡], Zeljko Uzelac[‡], Joan Gesmonde[§], Simon Bulling[‡], Thomas Stockner[‡], Michael Freissmuth[‡], Stefan Boehm[‡], Gary Rudnick[§], Harald H. Sitte[‡], and Walter Sandtner[‡1]

From the [‡]Center of Physiology and Pharmacology, Medical University of Vienna, A-1090 Vienna, Austria and the [§]Department of Pharmacology, Yale University School of Medicine, New Haven, Connecticut 06520-8066

Background: hSERT is a neurotransmitter transporter driven by ion gradients with electroneutral stoichiometry but rheogenic properties.
Results: hSERT displays coupled and uncoupled currents. The uncoupled current depends on internal K^+.
Conclusion: The conducting state of hSERT is in equilibrium with an inward facing K^+-bound state.
Significance: This study provides a framework for exploring transporter-associated currents.

Serotonin (5-HT) uptake by the human serotonin transporter (hSERT) is driven by ion gradients. The stoichiometry of transported 5-HT and ions is predicted to result in electroneutral charge movement. However, hSERT mediates a current when challenged with 5-HT. This discrepancy can be accounted for by an uncoupled ion flux. Here, we investigated the mechanistic basis of the uncoupled currents and its relation to the conformational cycle of hSERT. Our observations support the conclusion that the conducting state underlying the uncoupled ion flux is in equilibrium with an inward facing state of the transporter with K^+ bound. We identified conditions associated with accumulation of the transporter in inward facing conformations. Manipulations that increased the abundance of inward facing states resulted in enhanced steady-state currents. We present a comprehensive kinetic model of the transport cycle, which recapitulates salient features of the recorded currents. This study provides a framework for exploring transporter-associated currents.

Neurotransmitter transporters such as serotonin transporter (SERT),[2] dopamine transporter (DAT), and norepinephrine transporter (NET) are essential for synaptic transmission. SERT is responsible for serotonin (5-HT) reuptake from the synaptic cleft and therefore shapes synaptic transmission by both terminating receptor-mediated signaling events and by replenishing vesicular neurotransmitter pools (1). SERT is an important drug target for therapeutic compounds such as antidepressant 5-HT reuptake inhibitors and for illicit substances, such as cocaine and amphetamines including methylene-dioxymethamphetamine (ecstasy) (2).

A model of the SERT transport cycle was first derived from measuring the flux of radiolabled 5-HT and the influence of intracellular and extracellular ions. The salient features of this model posited that one Na^+ and one Cl^- ion were co-transported with the substrate and one K^+ ion was counter transported with each positively charged 5-HT molecule (3, 4). This stoichiometry predicts that no net charge movement occurs during the transport cycle. In contrast to this prediction, several studies showed that SERT mediates a constant current when challenged with the natural substrate 5-HT or with amphetamines (5–8). Single-channel recordings (9) and experiments measuring uptake and current simultaneously (5, 7), suggested that most if not all of the current was accounted for by uncoupled ion flux. In addition, the presence of a substrate-independent leak current further supports the notion that in SERT, ion permeation is not strictly coupled to transport.

Although SERT is the only neurotransmitter transporter for which transport stoichiometry is believed to be electroneutral, the presence of an uncoupled current component was also shown in DAT and NET (10–13). For example, in the case of DAT it was proposed that the contribution of the uncoupled current is responsible for approximately 50% of the current amplitude measured upon dopamine addition (14). With respect to these leak currents, which are uncoupled by definition, both DAT and NET are phenomenologically very similar to SERT. Because the uncoupled currents of SERT, DAT, and NET are not direct indicators of substrate transport, it has been difficult to use measurement of these currents to understand structural and mechanistic aspects of transport. The work presented here attempts to assign a mechanistic basis for these currents.

Additionally it is unclear why SERT, NET, or DAT would dissipate part of the energy stored in transmembrane ion gradients without obvious benefits for transport. However, there are indications that substrate-induced currents and reverse transport are correlated (15). In DAT a mechanism has been proposed in which substrate release is carried by a channel mode of the transporter (16). Also for SERT, it was suggested

* This work was supported, in whole or in part, by Fonds zur Förderung der Wissenschaftlichen Forschung Grants P18706 and SFB35-06 (to H. H. S.) and P17611 (to S. B.). This work was also supported by National Institutes of Health Grant DA007259 (to G. R.).
⌘ *Author's Choice*—Final version full access.
[S] This article contains supplemental Fig. 1.
[1] To whom correspondence should be addressed. Tel.: 43-1-4277-64188; Fax: 43-1-4277-9641; E-mail: walter.sandtner@meduniwien.ac.at.
[2] The abbreviations used are: SERT, serotonin transporter; DAT, dopamine transporter; h, human; 5-HT, serotonin; NET, norepinephrine transporter; NMDG, *N*-methyl-D-glucamine; MTSEA, 2-aminoethyl methanethiosulfonate hydrobromide.

that 5-HT is driven through a channel in the transporter by rheogenic Na^+ flux (17). However, this proposal is inconsistent with observations that imposing a membrane potential did not affect the rate or steady-state level of 5-HT uptake (3). Moreover, co-expression of syntaxin 1A eliminated 5-HT-induced and endogenous SERT currents but not the transport of 5-HT (7). There are reports that SERT and DAT currents are regulated *in vivo* by association with syntaxin (7, 18).

In the present study, we characterized the nature of the uncoupled currents. By combining electrophysiological, biochemical, and fluorescence microscopy techniques we show that the uncoupled current in SERT is carried by a K^+-dependent conducting state that is in equilibrium with an inward facing conformation of the transporter.

EXPERIMENTAL PROCEDURES

hSERT Expression in Xenopus Oocytes—Stage V and VI *Xenopus* oocytes were isolated from female frogs (NASCO, Ft. Atkinson, WI), washed with a solution containing 96 mM NaCl, 2 mM KCl, 20 mM $MgCl_2$, and 5 mM HEPES (titrated to pH 7.4 with NaOH), treated with 1 mg/ml collagenase for 0.5 to 1 h, and had their follicular cell layers manually removed. As judged from photometric measurements, ~5 ng of cRNA was injected into each oocyte with a Drummond microinjector (Broomall, PA). cRNA was synthesized using a T7 promoter cRNA synthesis kit (Ambion). *Xenopus laevis* oocytes were injected with 50-nl cRNAs of hSERT (5 ng/oocyte). Oocytes were allowed 3–5 days to express the hSERT before attempting recordings.

Two-electrode Voltage Clamp—Recordings were made in the two-electrode voltage clamp configuration using a TEC 10CD clamp (npi electronic, Tamm, Germany). Oocytes were placed in recording chambers in which the bath flow rate was about 100 ml/h, and the bath level was adjusted so that the total bath volume was <500 μl. Electrodes were filled with 3 M KCl and had resistances of less than 0.5 megohm. Using pCLAMP6 (Axon Instruments, Foster City, CA) software, data were acquired at 0.5 kHz after low pass filtration at 50 Hz. The recording solutions contained 100 mM NaCl, 2 mM KCl, 2 mM $CaCl_2$, 10 mM HEPES, pH 7.4. In Li^+ experiments NaCl was replaced by LiCl.

Whole Cell Patch Clamp—For patch clamp recordings, HEK293 cells stably expressing hSERT (hs4to) (8) were seeded at low density 24 h before the measurement. To measure substrate-induced hSERT currents cells were voltage clamped using the whole cell patch clamp technique. Briefly glass pipettes were filled with a solution consisting of 133 mM potassium gluconate, 5.9 mM NaCl, 1 mM $CaCl_2$, 0.7 mM $MgCl_2$, 10 mM HEPES, 10 mM EGTA, adjusted to pH 7.2 with 30 mM KOH. For some experiments the internal K^+ concentration had to be reduced. In these instances, the pipette solution consisted of 163 mM NMDG, 137 mM MES, 5.9 mM NaCl, 1 mM $CaCl_2$, 0.7 mM $MgCl_2$, 10 mM HEPES, 10 mM EGTA, pH 7.2. The cells were continuously superfused with external solution (140 mM NaCl, 3 mM KCl, 2.5 mM $CaCl_2$, 2 mM $MgCl_2$, 10 mM HEPES, 20 mM glucose, adjusted to pH 7.4 with NaOH).

Currents were recorded at room temperature (20–24 °C) using an Axopatch 200B amplifier and pClamp 10.2 software (MDS Analytical Technologies). Unless otherwise stated, cells were voltage clamped to a holding potential of −70 mV, and 5-HT was applied for 5 s once every 60 s. Current traces were filtered at 1 kHz and digitized at 2 kHz using a Digidata 1320A (MDS Analytical Technologies). Liquid junction potential was calculated to be 16 mV and was compensated. Drugs were applied using a DAD-12 (Adams and List, Westbury, NY), which permits complete solution exchange around the cells within 100 ms (19). Current amplitudes in response to 5-HT application were quantified using Clampfit 10.2 software. Passive holding currents were subtracted, and the traces were filtered using a 100-Hz digital Gaussian low pass filter. At potentials more positive than −20 mV a substantial background noise became detectable, which resulted from the activation of endogenous K^+ currents. Hence, it was necessary to reduce this noise by applying 5-HT three times for 5 s every minute at the same holding potential. At a given voltage, the peaks of the resulting traces were aligned, and traces were averaged before proceeding with the analysis. From each trace, we analyzed the peak current during the first 200 ms (peak) and the current within the last second of the substrate application (steady state).

FRET Measurements—Resonance energy transfer (FRET) measurements in HEK293 cells expressing fluorescently tagged hSERT were performed as described previously (20), using a Zeiss Axiovert 200 microscope. In brief, images were taken using a CCD camera (Coolsnap fx; Roper Scientific), a 63× NA 1.4 objective, and LUDL filter wheels allowing a rapid excitation and emission filter exchange. Background fluorescence was subtracted from all images. We analyzed the images pixel by pixel using National Institutes of Health ImageJ 1.43b with the plug-in PixFRET (21). Spectral bleed-through parameters for the donor bleed-through (DBT) and the acceptor (ABT) were determined, and NFRET was calculated according to Equation 1.

$$\mathrm{NFRET} = (I_{\mathrm{FRET}} - \mathrm{ABT} \times I_{\mathrm{Acc}} - \mathrm{DBT} \times I_{\mathrm{Don}}) / \sqrt{(I_{\mathrm{Don}} \times I_{\mathrm{Acc}})} \quad \text{(Eq. 1)}$$

For statistical comparison the mean NFRET was measured at the plasma membrane using the computed NFRET image.

Measurement of Cytoplasmic Pathway Accessibility—Membranes from HeLa cells expressing hSERT S277C in the X5C background (22, 23) were incubated in wells of Multiscreen-FB plates (Millipore, Bedford, MA), with the indicated concentrations of MTSEA and 5-HT or ibogaine for 15 min in a solution of 150 mM NaCl or LiCl buffered with 10 mM HEPES adjusted to pH 8.0 with NaOH or LiOH, respectively. Membranes were then washed by filtration with binding buffer (10 mM HEPES, adjusted to pH 8.0 with NaOH, 150 mM NaCl, 0.1 mM $CaCl_2$, and 1 mM $MgCl_2$) and assayed for binding of 2-β-carbomethoxy-3-β-(4-[^{125}I]iodophenyl)tropane (β-CIT) at 0.1 nM. After 1 h at room temperature, the membranes were washed three times with binding buffer. The amount of β-CIT bound was measured using a Wallac MicroBeta plate counter. Rate constants for inactivation were calculated from the MTSEA concentration leading to half-maximal inactivation (24).

Modeling—A kinetic model of SERT was developed which was based on a published model of DAT (25) but incorporated the differences in stoichiometry between the two transporters.

The time-dependent changes in state occupancies were evaluated by numerical integration of the resulting system of differential equations using GNU Octave 3.2.4. The rate constants used for the simulation were taken from the DAT model and modified to account for detailed balance and different affinities in our system. The voltage dependence of individual rates was modeled according to Ref. 26 assuming a symmetric barrier as $k_{ij} = k^0_{ij}\exp(-z_{Qi,j}FV/2RT)$, with $F = 96{,}485$ Coulombs·mol^{-1}, $r = 8.314$ JK^{-1}mol^{-1}, and V the membrane voltage in volts and $T = 293$ K. Coupled membrane currents in response to substrate application were calculated as $I = (-F\Sigma z_{Q,ij}(p_i k_{ij} - p_j k_{ji}))NC/N_A$, with $z_{Q,ij}$ being the net charge transferred during the transition, NC the number of transporters set to 4e6, and N_A 6.022e23. The uncoupled current was modeled as a current trough a Na^+-permeable channel with $I = P_c\gamma NC(V - V_{rev})$, with P_c being the occupancy of the channel state, γ the single-channel conductance of 2.4 picosiemens, NC the number of channels (4e6), V the membrane voltage, and V_{rev} the reversal potential of Na^+ being 80 mV. The extra- and intracellular ion concentrations were set to the values used in patch clamp experiments. To account for the noninstantaneous onset of substrate in patch clamp experiments we modeled the substrate application as exponential rise with a time constant of 20 ms.

Statistics—All values are given as mean ± S.E. if not stated otherwise. Affinity values obtained by nonlinear fits to a Hill equation are given as EC_{50} value with 95% confidence interval. The statistical significance of differences between groups were analyzed using Mann-Whitney *U* test or if applicable Kruskal-Wallis nonparametric ANOVA using Dunn's post hoc test. p values < 0.05 were considered statistically significant.

RESULTS

5-HT-induced Current of hSERT Has Two Components—hSERT currents were measured with the whole cell patch clamp technique in HEK293 cells stably expressing the transporter. To allow for the temporal resolution of current kinetics, 5-HT was applied with a rapid superfusion device with solution exchange times between 50 and 100 ms (see "Experimental Procedures").

Single cells were voltage clamped to −70 mV. As shown in Fig. 1*a*, low concentrations of 5-HT (<1 μM) induced currents with a slow onset and no sign of run-down during the application time of 5 s (this current is termed steady-state current throughout the subsequent description). This current is inwardly directed for negative potentials (with an estimated reversal potential of approximately 80 mV), indicating that most of the induced current was carried by Na^+. When the concentration of 5-HT was increased above 1 μM, an initial transient component was detected (termed peak current throughout the subsequent text). Whereas the steady-state component reached its maximum at 3 μM and accounted for −7.3 ± 1.2 pA, the peak amplitude increased further at higher concentrations of 5-HT. At 3 μM 5-HT the peak amplitude was −9.0 ± 1.5 pA, and at 100 μM 5-HT it was −11.3 ± 1.6 pA. The amplitude of the steady-state component was plotted as a function of the 5-HT concentration and fitted to a Hill equation. The EC_{50} was approximately 160 nM (Fig. 1*b*, *filled circles*). To fit the peak amplitudes we used a two-site binding model

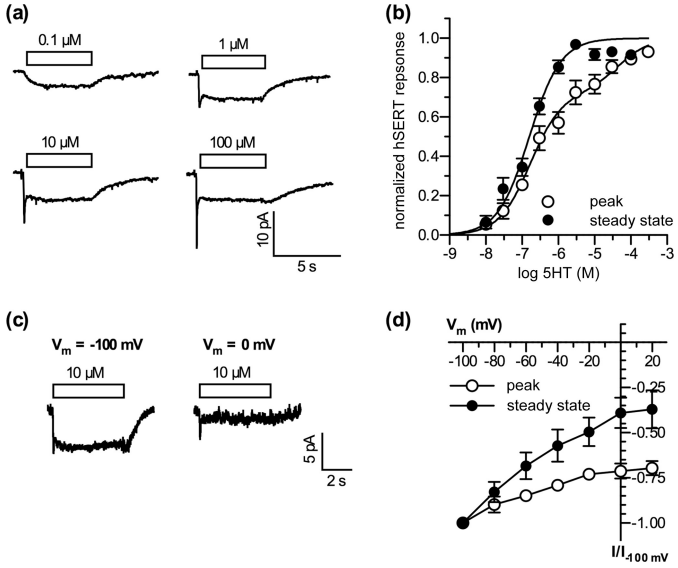

FIGURE 1. **5-HT-induced currents in hSERT-expressing cells have a transient and a steady-state component.** *a*, sample currents recorded at a holding potential of −70 mV. 5-HT was applied at the indicated concentrations. *b*, concentration response curves for the peak (*open symbols*) and the steady-state component (*filled symbols*) of the hSERT current response. *Solid lines* depict the nonlinear least square fit to the data (single affinity for steady state, dual affinity for peak). The best fit values obtained were: steady state, EC_{50} = 159.5 nM (114.8–221.5 nM; $n_H = 1$, $n = 12$ cells); peak, $EC_{50}(1) = 168.7$ nM (113.2–250.6 nM), $EC_{50}(2) = 45.5$ μM (15.9–130.6 μM), $n_H(1,2) = 1$. *c*, sample currents recorded at a holding potential of either −100 mV (*left*) or 0 mV (*right*). 5-HT (10 μM) was applied as indicated. *d*, current to voltage relation for the peak (*open symbols*) and the steady-state component (*filled symbols*) of the hSERT current recorded in response to 10 μM 5-HT.

because below 1 μM 5-HT, the earliest current measurements contain contributions from both peak and steady-state currents. This fit yielded a EC_{50} of approximately 170 nM for the first component and 45 μM for the second component (Fig. 1*b*, *open circles*).

In addition to the differences in time dependence and amplitude between the two 5-HT-induced currents, their voltage dependences also differed. SERT-expressing cells were voltage clamped to different holding potentials, and substrate current was induced with 10 μM 5-HT. The peak current was only modestly affected by an increase in clamp voltage from −100 to +20 mV, *e.g.* the amplitude was reduced by less than 30% ($n = 7$). In contrast, over the same voltage range the steady-state component was reduced by >60% ($n = 7$, Fig. 1, *c* and *d*). When the cells were clamped to holding potentials more positive than 0 mV the background noise increased due to activation of endogenous K^+ channels, and noise precluded reliable analysis of current amplitudes.

These data demonstrate the presence of two different components in 5-HT-induced currents of hSERT. One component is transient and saturates only at high 5-HT concentration whereas the other saturates at low 5-HT and has a slow rise time and no decay.

Conducting State Is Linked to K^+—Intracellular K^+ plays an important role in the function of hSERT (3, 4). The replacement of intracellular K^+ with other cations led to a dramatic decrease in 5-HT uptake. Similarly, omission of intracellular K^+ reduced the amplitude of hSERT currents recorded from *X. laevis* oocytes (6). Due to the large size and the slow exchange rate of

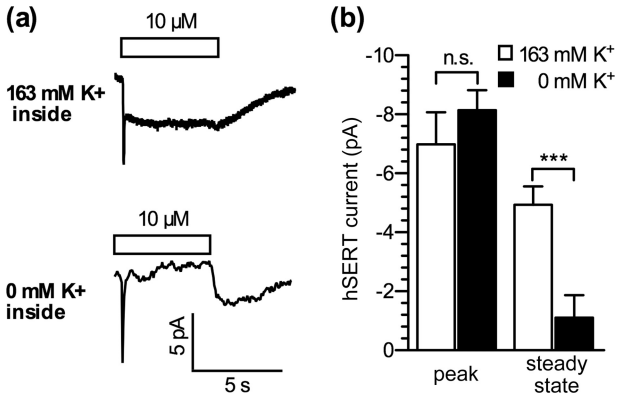

FIGURE 2. **Low intracellular K^+ abolishes the steady-state component of the 5-HT-induced current in hSERT.** Single HEK293 cells stably expressing hSERT were voltage clamped to a holding potential of −70 mV, and 5-HT (10 μM) was applied. *a*, sample currents from two cells recorded either with 163 mM K^+ (*upper*) or 0 mM (substituted with NMDG; *lower*) in the pipette solution. *b*, statistical evaluation of peak and steady-state component at the indicated conditions (163 K^+ *versus* 0 K^+). Peak, −7.0 ± 1.1 pA *versus* −8.1 ± 0.7 pA; steady state, −4.9 ± 0.6 pA *versus* −1–1 ± 0.8 pA. ***, $p < 0.001$, *n.s.*, not significant, Mann-Whitney *U* test, $n = 13$).

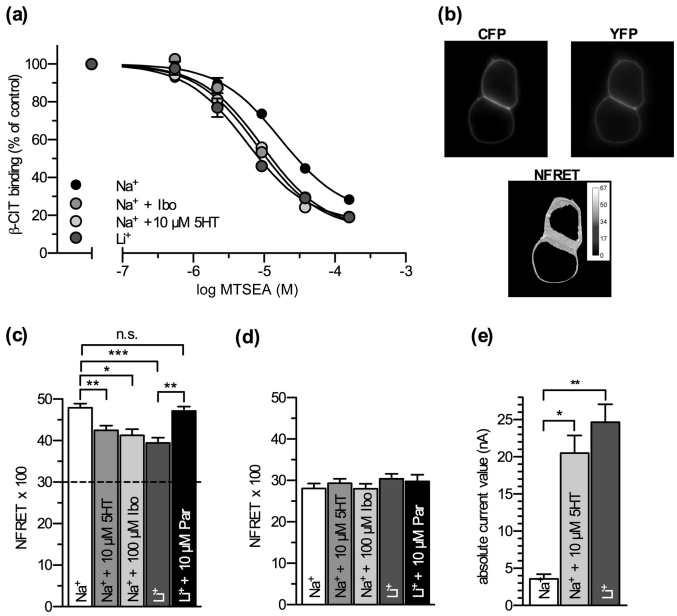

FIGURE 3. **Conformational probes indicate that ibogaine, 5-HT, and Li^+ favor the inward facing conformation of SERT.** *a*, membranes from HeLa cells transfected with SERT S277C in the X5C background were treated for 15 min with the indicated concentrations of MTSEA either in the presence of 150 mM Na^+ alone or with 40 μM ibogaine, 10 μM 5-HT, or after substitution of Na^+ with Li^+. The log IC_{50} values for MTSEA for all of the above treatments were shifted to the left compared with Na^+ (Na^+, 17.2 μM (12.8–23.0 μM); 5-HT, 8.2 μM (6.7–10.2 μM); ibogaine (9.6 μM (7.3–12.6 μM)), Li^+, 5.8 μM (4.4–7.6 μM)). *b*, example images taken of HEK293 cells transiently transfected with a hSERT construct tagged with ECFP at the N terminus and EYFP at the C terminus recorded at the indicated filter settings. *c*, calculated NFRET values. Addition of 5-HT or ibogaine to a Na^+-containing bath solution as well as exchange of Na^+ for Li^+ significantly reduce NFRET. The latter effect is rescued by the addition of 10 μM paroxetine to the bath solution (Na^+, 47.9 ± 1.0; 5-HT, 42.5 ± 1.1; ibogaine, 41.3 ± 1.5; Li^+, 39.5 ± 1.2; Li^+ + paroxetine, 47.2 ± 1.0). *, $p < 0.05$; **, $p < 0.01$; ***, $p < 0.001$, $n = 21$–109, Kruskal-Wallis with Dunn's post hoc test). The *dashed line* marks the contribution level of intermolecular FRET as determined in *d*. *d*, calculated NFRET values from HEK293 cells transiently transfected with two hSERT constructs tagged with either ECFP or EYFP at the N terminus ($p > 0.05$, $n = 40$ each, Kruskal-Wallis test). *e*, single hSERT expressing *X. laevis* oocytes were voltage clamped to −40 mV using the two-electrode voltage clamp technique and continuously superfused with bath solution. Absolute current values are plotted. Addition of 10 μM 5-HT to a Na^+-containing bath solution as well as the exchange of Na^+ for Li^+ significantly increase the current amplitude (Na^+, 3.6 ± 0.7 nA; 5-HT, 20.5 ± 2.4 nA; Li^+, 24.7 ± 2.4 nA. **, $p < 0.01$, $n = 6$, Kruskal-Wallis test with Dunn's post hoc test).

solution around the cells, currents recorded in oocytes most likely represent only the steady-state component. In the cellular system used here, the steady-state current in response to 10 μM 5-HT was also abolished when K^+ was replaced by NMDG. In contrast, the peak current remained unaltered (Fig. 2). These data show that the steady-state component requires internal K^+, whereas the peak component does not, suggesting that they represent different processes.

Conducting State Is Entered via an Inward facing Conformation—The peak current may reflect a stoichiometric transfer of net charge during the conformational transition between the outward and the inward facing conformations as 1 Na^+, 1 Cl^-, and 1 5-HT^+ are translocated across the membrane (4, 27). However, this transition is followed by the compensating translocation of 1 K^+ outward as SERT returns to its initial conformation, resulting in an electroneutral stoichiometry (3, 4) that does not account for the steady-state current observed here. Li^+ induces a large leak current in hSERT, even in the absence of 5-HT (5). The underlying cause of this Li^+ current has remained enigmatic. However, Lin *et al.* (9) found single channels in *X. laevis* oocytes expressing hSERT that opened more frequently in the presence of Li^+ but retained the same single-channel conductance and mean open time. Together with the finding that Li^+ altered SERT conformation (28), these results suggest that the Li^+-induced current could be due to a change in the conformational equilibrium that increased the probability of conducting state rather than enhanced Li^+ permeation relative to Na^+.

To understand the relationship between conformational equilibrium and the induction of various currents, we employed conformational probes that monitor the relative proportion of inward and outward facing states. A conformational mechanism of SERT has been proposed that involves reorientation of a four-helix bundle containing transmembranes 1, 2, 6, and 7 relative to the rest of the protein (29). This movement closes an aqueous pathway leading from the cell exterior to the substrate binding site and concomitantly opens a pathway from the binding site to the cytoplasm, increasing the accessibility of residues lining the cytoplasmic pathway. To measure this accessibility change we used membranes from cells expressing a SERT mutant with a single reactive cysteine in the cytoplasmic permeation pathway (SERT-*X*5C/S277C). This construct was previously shown to react more rapidly with MTSEA when the transporter was in an inward facing conformation (23). Under control conditions (150 mM Na^+, Fig. 3*a*, *black circles*) the calculated reaction rate for MTSEA labeling was 43.2 ± 1.7 $s^{-1}\,M^{-1}$. The plant alkaloid ibogaine stabilizes an inward facing conformation of hSERT (30, 31). In the presence of ibogaine (40 μM) and Na^+, the labeling rate increased >3-fold. Agents known to increase the current amplitude such as 5-HT and Li^+ also increased the reaction rate, indicating a more open cytoplasmic pathway. 10 μM 5-HT (Fig. 3*a*, *light gray circles*) increased the rate of labeling >2.5-fold, and exchanging Na^+ with Li^+ (Fig. 3*a*, *dark gray circles*) increased the rate >4-fold.

These data show that both 5-HT and Li^+ increase the rate of labeling to an extent comparable with ibogaine, implying that they favor accumulation of SERT in an inward facing conformation.

We confirmed this interpretation by using a double-tagged hSERT construct, in which a fluorescence donor (ECFP) and acceptor (EYFP) were attached to the N and C terminus, respectively. This construct (termed CSERTY) allows for measuring intramolecular distances within SERT by FRET (Fig. 3*b*) (32). Because the N terminus is attached to the four-helix bundle of SERT, reorientation of the bundle to open the cytoplasmic pathway increases the distance between the N and C termini (29), and the FRET intensity is therefore sensitive to the conformation of SERT (Fig. 3*c*) (31). NFRET (see definition under "Experimental Procedures") in 140 mM Na^+ (Fig. 3*c*, *white bar*) was significantly reduced by the addition of 10 μM 5-HT (Fig. 3*c*, *light gray bar*). Likewise, ibogaine reduced NFRET to the same extent as 5-HT (Fig. 3*c*, *mid gray bar*). Moreover, replacement of external Na^+ with Li^+ decreased NFRET to identical values (Fig. 3*c*, *dark gray bar*). The decrease in FRET signal is consistent with separation of the N and C termini from each other as the cytoplasmic pathway opens. The Li^+-induced drop in FRET was prevented by the addition of 10 μM paroxetine, a competitive inhibitor like others that are known to stabilize the transporter in the outward facing conformation (33, 34) (Fig. 3*c*, *black bar*). An alternative interpretation is to assume that the addition of CFP and YFP at the C terminus and N terminus, respectively, alters the protein conformation and in a way that renders the external binding site less accessible. This is, however, unlikely because it would change the turnover rate and the binding kinetics of CSERTY. In fact, both substrate uptake and inhibitor binding by CSERTY are indistinguishable from wild-type SERT (32). This suggests that the fluorescent protein moieties do not impose a steric constraint on the helical portion of the transporter.

Because transporters of the SLC6 family are known to form oligomers (35–37), intermolecular FRET can also occur (32), thereby obscuring the relationship between conformational rearrangements and the FRET signal. We estimated the contribution of intermolecular FRET by co-expressing two SERT constructs, one with an N-terminal ECFP and one with a C-terminal EYFP, in HEK293 cells. Under these conditions NFRET values of around 30 were measured. In contrast to the double-tagged construct, these values were not significantly affected by the different treatments (see Fig. 3*d*). Accordingly, we consider it unlikely that intermolecular FRET contributes to the changes observed with ibogaine, 5-HT and Li^+.

Evaluation of Current Amplitudes—We also expressed hSERT in *X. laevis* oocytes to study steady-state current amplitudes. Addition of 5-HT (10 μM) in 100 mM Na^+, as shown in Fig. 3*d*, led to a >5-fold increase in current amplitude at a holding potential of −40 mV (Fig. 3*d*, *light gray bar*). When Na^+ was replaced with 100 mM Li^+ (Fig. 3*d*, *dark gray bar*), the holding current was also enhanced almost 7-fold. The Na^+ leak was defined by its sensitivity to blockade by 10 μM paroxetine. Although ibogaine was effective in changing the conformation of hSERT (Fig. 3, *a* and *c*), it did not induce a current in *X. laevis* oocytes (supplemental Fig. 1).

Kinetic Model Describing Function of hSERT—Taken together, the data summarized above are consistent with the hypothesis that the uncoupled conductance of SERT requires an inward facing conformation of the transporter bound to K^+. We developed a mathematical model for SERT-mediated 5-HT transport and ionic currents, which is represented in Fig. 4*a*. In this model, the peak current is due to a synchronized conformational change that results from 5-HT addition to outward facing SERT molecules (T_oNaCl in Fig. 4*a*). The steady-state current is modeled to occur with formation of T_iK_{Cond}, a conductive species transiently formed from the inward facing conformation with K^+ bound (T_iK, Fig. 4*a*). Membrane currents were modeled as the linear sum of the coupled transport (peak) component and the uncoupled current. We tested the ability of the model to recapitulate our experimental findings. As demonstrated in Fig. 4, *b* and *c*, the model is capable of reproducing the hallmarks of the response of hSERT currents measured in HEK293 cells to 5-HT concentration.

The simulated *traces* in Fig. 4*b* show only a slowly activating current at lower 5-HT concentrations and a transient peak only at higher concentrations. Our model (Fig. 4*a*) provides an explanation for the different concentration dependences for the steady-state and peak components. External 5-HT controls the rate of formation of T_oNaSCl. At low 5-HT, this species is converted to T_iNaSCl by conformational change as fast as it is formed. The slow step in the overall cycle is the reverse conformational change T_iK to T_oK. Thus, at low 5-HT, most of the transporter will build up in the T_iK form, which is in equilibrium with the conducting species, T_iK_{Cond}. At high 5-HT, T_oNaSCl forms faster than it can be converted to T_iNaSCl. Because the peak current results from this conformational transition, synchronized by addition of 5-HT to transporters essentially all waiting in the T_oNaCl state, the peak current is maximal only at 5-HT concentrations well above 1 μM, high enough to convert all the T_oNaCl to T_oNaSCl before a significant amount of T_oNaSCl is converted to T_iNaSCl. These concentrations are much higher than required to saturate the rate of the overall transport reaction or the uncoupled current, both of which are dependent on the concentration of T_iK.

The analysis of the concentration response relationship yields a EC_{50} of 106 nM for the steady-state current and 66 μM for the peak current, affinities very similar to those measured in HEK293 cells (Fig. 4*c*). Because the model predicts the peak and steady-state currents independently, the simulated 5-HT dependence of the peak current is not subject to a contribution from the uncoupled current. This analysis contrasts with Fig. 1*b* where the currents measured shortly after 5-HT addition are a mixture of peak and steady state. Therefore, the right shift in EC_{50} between the steady-state (uncoupled) and peak (coupled) currents is more clearly visible in Fig. 4*c*.

The model also emulates the voltage and K^+ dependence of each current. As depicted in Fig. 4, *d* and *e*, the model predicts a much stronger voltage dependence for the steady-state component relative to the peak component. This is reflected by a reduction in amplitude of almost 80% when stepping from −100 to 0 mV. In contrast, the peak component was reduced by only 35%. The predicted effect of removing internal K^+ was also similar to the observation in HEK293 cells (compare Figs. 2*a*

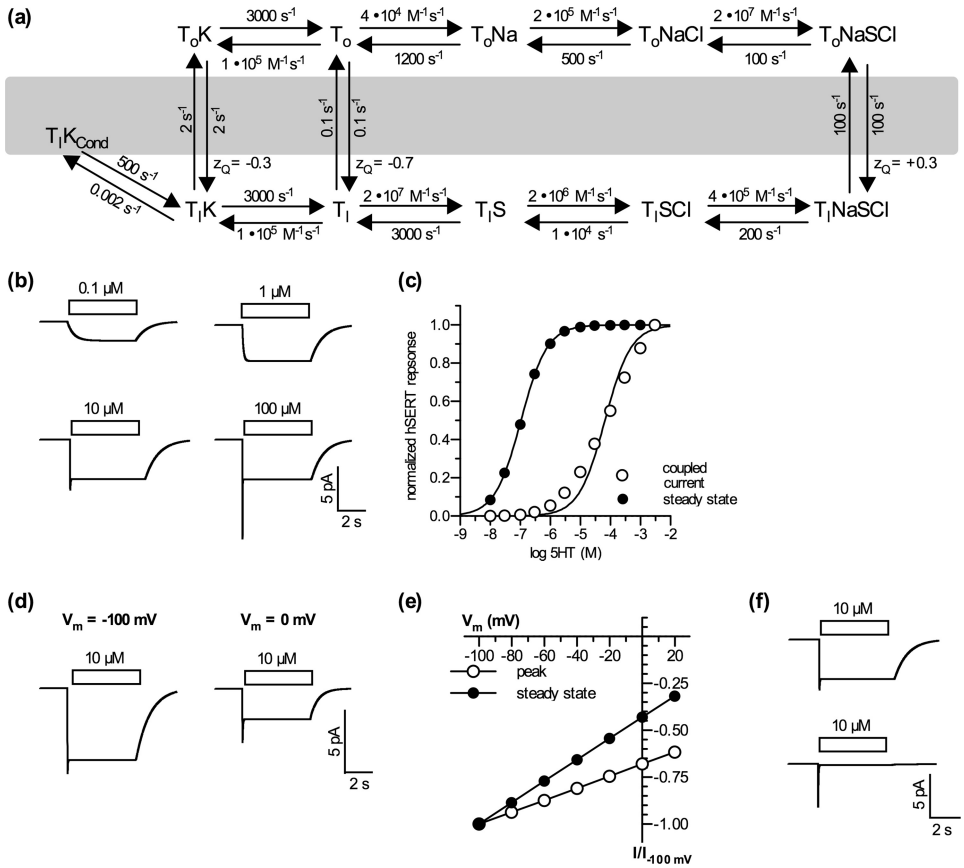

FIGURE 4. **Simulated substrate-induced currents are in good agreement with the data obtained in voltage clamp experiments.** *a*, alternating access model of hSERT. *b*, sample currents at different concentrations of 5-HT simulated with the kinetic model using a holding potential of −70 mV. *c*, concentration response relation of the coupled (*open circles*) and steady-state component (*filled circles*) of simulated hSERT currents. *Solid lines* depict the nonlinear least square fit to the data. The best fit values obtained were: steady state, EC_{50} = 105.9 nM (104.1–107.8 nM); coupled current, EC_{50} = 66.1 µM (47.0–92.8 µM). *d*, sample currents simulated at a holding potential of −100 mV (*left*) or 0 mV (*right*). *e*, simulated current-voltage relation of the coupled current (*open circles*) and steady-state component (*filled circles*). *f*, effect of internal K^+ on the steady-state component of simulated hSERT currents.

and 4*f*). Omission of internal K^+ in the model completely suppresses the steady-state component but does not affect the peak current.

Finally, we note that for simplicity we chose to model Na^+ and 5-HT binding to occur in a sequential order. However, there is strong evidence that 5-HT can bind in the absence of Na^+ (38). A second simplification was not to indicate H^+ antiport, which is assumed to occur in the absence of K^+ (4, 27) and is represented in Fig. 4*a* by the T_i to T_o transition. Both simplifications are justified by the reason that they do not affect the ability of the model to account for the SERT currents.

DISCUSSION

Secondary transporters such as hSERT couple the energy stored in ion gradients to the translocation of substrate and thus drive substrate energetically uphill against a concentration gradient. The conformational rearrangements required for transport are thought to occur as originally posited by the alternating access model: substrate binding to an outward facing conformation of the transporter initiates the transition to an inward facing conformation (39, 40). Following the release of substrate, the empty transporter returns to the outward facing conformation and thereby completes the kinetic cycle.

Numerous electrophysiological studies demonstrated currents through SERT (5–8), including a 5-HT-induced inward current, a substrate-independent leak current in Na^+ and Li^+, and a resistive transient current elicited by voltage jumps from positive (~ +40 mV) to negative membrane potentials (~−140 mV). Originally, Lester and co-workers speculated on the mechanistic basis of the currents by proposing a model in which the transporter occasionally adopted a channel-like conformation at conformational transition points of the cycle (5). The model envisaged that both outer and inner gates may be simultaneously open when the transporter converts between the outward and inward facing conformations (steps T_oNaSCl to T_iNaSCl and T_iK to T_oK in Fig. 4*a*).

Our analysis allows us to refine this view and to propose that the uncoupled current is carried by a species that is transiently formed from, and in equilibrium with, an inward facing SERT conformation with K^+ bound (T_iK in Fig. 4*a*). This conclusion is based on the following observations: (i) Two independent measurements of conformational equilibrium, FRET between N and C termini and accessibility of a cysteine residue in the cytoplasmic permeation pathway, indicate that increased uncoupled current follows an increase in the abundance of SERT in inward facing conformations. In contrast, conditions that favor an outward facing conformation, *i.e.* Na^+ and the presence of a competitive inhibitor such as paroxetine, support little or no current. (ii) In agreement with Adams and DeFelice

(6) we also found that the steady current required internal K^+. Together, these observations suggest that the conducting state requires formation of the K^+-bound, inward facing conformation. (iii) A plausible kinetic model consistent with previous observations recapitulates the properties of peak and steady-state currents, including differences in their voltage and concentration dependence and kinetics.

Ibogaine increased accessibility of the cytoplasmic pathway and decreased FRET between the N and C termini, but did not activate the uncoupled current. Thus, although the inward facing conformation may be required for this current, it is not itself sufficient. Ibogaine is likely to bind to the substrate site of SERT; indeed, the structure of 5-HT is contained within the ibogaine molecule (30). Thus, the ibogaine-bound SERT complex is likely to resemble T_INaSCl in Fig. 4*a*, which cannot bind K^+ and therefore does not mediate the uncoupled current. Other explanations for the absence of ibogaine-induced currents are that ibogaine may directly block the conduction pathway or it may stabilize a different inward facing conformation of the transporter that is not in equilibrium with the conducting state.

The conducting state was used as a reference point to construct a comprehensive kinetic model describing transport and current. Kinetic information was extracted from published transport rates and binding studies. We found it necessary to include 10 individual states to account for the stoichiometry of the transporter. We rigorously tested this model with our experimental data, including the kinetics of the recorded currents, their voltage dependence, and their response to 5-HT concentration. The model summarized in Fig. 4*a* not only recapitulates our measurements and published findings but also provides a framework for exploring the nature of the 5-HT-induced current and of the substrate-independent leak currents (*e.g.* the Li^+ leak and the Na^+ leak). Previously, these currents were ascribed to independent activities of SERT (5) and of other transporters (14, 42). However, our analysis suggests that all currents may be carried by the same state which is in equilibrium with the inward facing, K^+-bound conformation. This state may represent the conductance observed by Lester and co-workers as single-channel openings (9). Thus, our comprehensive model provides for a unifying concept of transporter-associated currents. Support for this view comes from observations that treatments that eliminate the 5-HT-induced current (removal of internal K^+ (6) and co-expression of syntaxin 1a (7)) also eliminate Li^+-induced currents. Furthermore, internal K^+ was required for uncoupled currents initiated by both 5-HT and Li^+ (see Ref. 6 and Fig. 2*a*), suggesting that the transition to an inward facing state was not sufficient unless it resulted in K^+ binding. Additionally, identification of the conducting species of SERT and the conformational transitions leading to stoichiometric (peak) currents allows the use of these currents to investigate the mechanism of SERT-mediated transport.

Finally, our model provides an explanation for the inwardly directed current peak observed upon fast application of 5-HT onto cells expressing SERT. We surmise that the current peak is capacitive in nature and a consequence of the electrogenic transition that carries substrate and ions through the cell membrane. A similar observation was reported for DAT challenged by fast perfusion with D-amphetamine (25). However, because the stoichiometry in DAT was assumed to be electrogenic, Erreger *et al.* modeled the steady-state current as strictly coupled. In contrast to DAT, the established stoichiometry in SERT and a large body of experimental evidence indicate that the steady-state current is uncoupled.

Structural models are available that provide snapshots of conformations that occur during the kinetic cycle of transporters: the pertinent structural model for SERT is $LeuT_{Aa}$, which exists in at least two different conformations (43). Our results provide limited guidance in searching for the structural equivalent of the conducting state. A recent study by Zhao and Noskov (44) suggests the presence of a water wire from the cytoplasm to the Na2 site in the occluded state of $LeuT_{Aa}$. Limited conformational changes could conceivably open a potential pathway like this enough to conduct cations, possibly initiated by K^+ binding to the Na2 site. Our observations and others (6) link formation of the conducting state to binding of K^+. However a K^+ binding site does not exist in $LeuT_{Aa}$, and thus its location is still unknown. Additionally, there are apparent differences in the action of Li^+ on $LeuT_{Aa}$ and SERT. In $LeuT_{Aa}$, unlike SERT, Li^+ leads to the closure of the inner gate, favoring an outward facing conformation (45).

Our observations do not exclude the possibility that the conducting state can also be entered from the outward facing conformation with K^+ bound. With physiological ion gradients and in the presence of external 5-HT, the inward facing K^+-bound state is highly populated, whereas the K^+-bound outward facing conformation is rarely occupied. Future experiments will address whether the conducting state can also be entered from the K^+-bound outward facing conformation; this might be possible following an approach shown for EAAC1, where substrate gradient and all ion gradients are reversed for current measurements (46). Such a condition would populate the K^+-bound outward facing conformation, and this could therefore be a suitable way to address this question.

In conclusion, our approach highlights the usefulness of electrophysiological recordings to refine kinetic models. The time resolution of electrophysiology is high accordingly, currents are rich in detailed kinetic information, which is inaccessible to substrate flux measurements. Electrophysiology can be complemented with simultaneously recorded intramolecular measurements of distance changes with FRET (41). This provides structural reference points to constrain further studies. The feasibility of this strategy is currently being explored.

Acknowledgment—We thank Sacrament of Transition (Maribor, Slovenia) for the ibogaine.

REFERENCES

1. Kanner, B. I., and Zomot, E. (2008) *Chem. Rev.* **108,** 1654–1668
2. Seidel, S., Singer, E. A., Just, H., Farhan, H., Scholze, P., Kudlacek, O., Holy, M., Koppatz, K., Krivanek, P., Freissmuth, M., and Sitte, H. H. (2005) *Mol. Pharmacol.* **67,** 140–151
3. Rudnick, G., and Nelson, P. J. (1978) *Biochemistry* **17,** 4739–4742
4. Nelson, P. J., and Rudnick, G. (1979) *J. Biol. Chem.* **254,** 10084–10089
5. Mager, S., Min, C., Henry, D. J., Chavkin, C., Hoffman, B. J., Davidson, N., and Lester, H. A. (1994) *Neuron* **12,** 845–859

6. Adams, S. V., and DeFelice, L. J. (2003) *Biophys. J.* **85,** 1548–1559
7. Quick, M. W. (2003) *Neuron* **40,** 537–549
8. Hilber, B., Scholze, P., Dorostkar, M. M., Sandtner, W., Holy, M., Boehm, S., Singer, E. A., and Sitte, H. H. (2005) *Neuropharmacology* **49,** 811–819
9. Lin, F., Lester, H. A., and Mager, S. (1996) *Biophys. J.* **71,** 3126–3135
10. Ingram, S. L., Prasad, B. M., and Amara, S. G. (2002) *Nat. Neurosci.* **5,** 971–978
11. Carvelli, L., McDonald, P. W., Blakely, R. D., and Defelice, L. J. (2004) *Proc. Natl. Acad. Sci. U.S.A.* **101,** 16046–16051
12. Galli, A., Petersen, C. I., deBlaquiere, M., Blakely, R. D., and DeFelice, L. J. (1997) *J. Neurosci.* **17,** 3401–3411
13. Galli, A., DeFelice, L. J., Duke, B. J., Moore, K. R., and Blakely, R. D. (1995) *J. Exp. Biol.* **198,** 2197–2212
14. Sonders, M. S., Zhu, S. J., Zahniser, N. R., Kavanaugh, M. P., and Amara, S. G. (1997) *J. Neurosci.* **17,** 960–974
15. Sitte, H. H., Huck, S., Reither, H., Boehm, S., Singer, E. A., and Pifl, C. (1998) *J. Neurochem.* **71,** 1289–1297
16. Kahlig, K. M., Binda, F., Khoshbouei, H., Blakely, R. D., McMahon, D. G., Javitch, J. A., and Galli, A. (2005) *Proc. Natl. Acad. Sci. U.S.A.* **102,** 3495–3500
17. Petersen, C. I., and DeFelice, L. J. (1999) *Nat. Neurosci.* **2,** 605–610
18. Carvelli, L., Blakely, R. D., and DeFelice, L. J. (2008) *Proc. Natl. Acad. Sci. U.S.A.* **105,** 14192–14197
19. Boehm, S. (1999) *J. Neurosci.* **19,** 737–746
20. Bartholomäus, I., Milan-Lobo, L., Nicke, A., Dutertre, S., Hastrup, H., Jha, A., Gether, U., Sitte, H. H., Betz, H., and Eulenburg, V. (2008) *J. Biol. Chem.* **283,** 10978–10991
21. Feige, J. N., Sage, D., Wahli, W., Desvergne, B., and Gelman, L. (2005) *Microsc. Res. Tech.* **68,** 51–58
22. Zhang, Y. W., and Rudnick, G. (2005) *J. Biol. Chem.* **280,** 30807–30813
23. Zhang, Y. W., and Rudnick, G. (2006) *J. Biol. Chem.* **281,** 36213–36220
24. Rudnick, G. (2002) in *Transmembrane Transporters* (Quick, M. W., ed) pp. 125–141, Wiley-Liss, Hoboken, NJ
25. Erreger, K., Grewer, C., Javitch, J. A., and Galli, A. (2008) *J. Neurosci.* **28,** 976–989
26. Laeuger, P. (1991) *Electrogenic Ion Pumps*, Sinauer Associates, Sunderland, MA
27. Keyes, S. R., and Rudnick, G. (1982) *J. Biol. Chem.* **257,** 1172–1176
28. Ni, Y. G., Chen, J. G., Androutsellis-Theotokis, A., Huang, C. J., Moczydlowski, E., and Rudnick, G. (2001) *J. Biol. Chem.* **276,** 30942–30947
29. Forrest, L. R., Zhang, Y. W., Jacobs, M. T., Gesmonde, J., Xie, L., Honig, B. H., and Rudnick, G. (2008) *Proc. Natl. Acad. Sci. U.S.A.* **105,** 10338–10343
30. Jacobs, M. T., Zhang, Y. W., Campbell, S. D., and Rudnick, G. (2007) *J. Biol. Chem.* **282,** 29441–29447
31. Sucic, S., Dallinger, S., Zdrazil, B., Weissensteiner, R., Jørgensen, T. N., Holy, M., Kudlacek, O., Seidel, S., Cha, J. H., Gether, U., Newman, A. H., Ecker, G. F., Freissmuth, M., and Sitte, H. H. (2010) *J. Biol. Chem.* **285,** 10924–10938
32. Just, H., Sitte, H. H., Schmid, J. A., Freissmuth, M., and Kudlacek, O. (2004) *J. Biol. Chem.* **279,** 6650–6657
33. Tao, Z., Zhang, Y. W., Agyiri, A., and Rudnick, G. (2009) *J. Biol. Chem.* **284,** 33807–33814
34. Tavoulari, S., Forrest, L. R., and Rudnick, G. (2009) *J. Neurosci.* **29,** 9635–9643
35. Kilic, F., and Rudnick, G. (2000) *Proc. Natl. Acad. Sci. U.S.A.* **97,** 3106–3111
36. Schmid, J. A., Scholze, P., Kudlacek, O., Freissmuth, M., Singer, E. A., and Sitte, H. H. (2001) *J. Biol. Chem.* **276,** 3805–3810
37. Hastrup, H., Karlin, A., and Javitch, J. A. (2001) *Proc. Natl. Acad. Sci. U.S.A.* **98,** 10055–10060
38. Humphreys, C. J., Wall, S. C., and Rudnick, G. (1994) *Biochemistry* **33,** 9118–9125
39. Patlak, C. S. (1957) *Bull. Math. Biophys.* **19,** 209–235
40. Jardetzky, O. (1966) *Nature* **211,** 969–970
41. Sandtner, W., Bezanilla, F., and Correa, A. M. (2007) *Biophys. J.* **93,** L45–47
42. Andrini, O., Ghezzi, C., Murer, H., and Forster, I. C. (2008) *Channels* **2,** 346–357
43. Krishnamurthy, H., Piscitelli, C. L., and Gouaux, E. (2009) *Nature* **459,** 347–355
44. Zhao, C., and Noskov, S. Y. (2011) *Biochemistry* **50,** 1848–1856
45. Zhao, Y., Terry, D. S., Shi, L., Quick, M., Weinstein, H., Blanchard, S. C., and Javitch, J. A. (2011) *Nature* **474,** 109–113
46. Zhang, Z., Tao, Z., Gameiro, A., Barcelona, S., Braams, S., Rauen, T., and Grewer, C. (2007) *Proc. Natl. Acad. Sci. U.S.A.* **104,** 18025–18030